JISSE
ISSN: 2636-4425

Journal of International Society for Science and Engineering
Vol. 5, No. 4, 19-27 (2023)

JISSE
E-ISSN:2682-3438

CFD Simulation with Experimental Validation for Heavy Oil-Water Flow in Horizontal Pipe

Mohamed H. Alashker[1,*], Ali A. Zahran[1], Mohamed E. Elrefaie[2], Ali Abuelezz[3]

[1] *Volume and Fluid Flow Metrology Laboratory, National Institute of Standards (NIS), Giza, Egypt*

[2] *Department of Mechanical Engineering, Faculty of Engineering, Al-Azhar University, Cairo, Egypt*

[3] *Materials and Force Metrology Laboratory, National Institute of Standards (NIS), Giza, Egypt*

ARTICLE INFO

Article history:
Received:
Accepted:
Online:

Keywords:
CFD simulation
Phase holdup
Kelvin-Helmholtz instability
Interface tracking
VOF scheme
Oil-water flow

ABSTRACT

Deep knowledge of two-phase oil-water flow behavior through horizontal pipelines is crucial for transportation network design. In particular, the behavior of core annular flow (CAF) pattern where oil flows as the core fluid and water flows as an annular fluid. A three-dimensional model of transient isothermal flows in a horizontal pipe was created using CFD code ANSYS FLUENT 2020 R1 applying an explicit Volume of Fluid (VOF) scheme. CFD simulation study was performed on heavy oil-water CAF flow and validated with the experimental study. CAF pattern was determined during numerical runs conducted at various mixture superficial velocities. Thicker eccentricity core flow has been observed numerically and consistent with the flow visualization observed experimentally. The interfacial waves appeared in the simulation study during the flowing due to Kelvin-Helmholtz instability. The simulated oil holdup and transient pressure were found to be in reasonable agreement level with Areny's holdup correlation predictions and experimental results, respectively. This investigation further demonstrates that the CFD model may predict the hydrodynamic behavior of CAF to a satisfactory level.

1. Introduction

The design of the oil transportation network pipeline is a vital issue to pump heavy oil downstream after it is lifted to the wellhead surface. The demand for heavy oil transportation has increased over the last few decades because heavy oil reserves are available in many countries, while reserves of light oils are depleted [1], [2].

The viscous drag and wall friction which results in a high pressure drop in the pipeline are much higher in the heavy oil compared to conventional light oils [3]. As such, without prior reduction in the heavy crude oil viscosity, transportation is almost impossible. This is because of the enormous power requirement to overcome the high pressure drop in the pipeline owing to its high viscosity [4].

Applying the CAF technique is a promising solution to overcome the challenges of transporting heavy oil without changing the physical properties. CAF is the one of flow patterns observed in the two-phase flow of heavy oil-water via pipelines. The oil of high viscosity flows as the core fluid and surrounded by the water film of low viscosity flows as an annular fluid. This results in reduced wall shear stresses and significantly decreased pressure gradient. The CAF pattern is affected by several parameters, such as the viscosity and density of oil, the phase holdup, the flow shear rate and the interfacial tension, [5]. In the two-phase oil-water properties, the viscosity difference is highly great, and the density difference is relatively small.

The phase holdup, denoting the in-situ volume fraction of a specific phase, plays a crucial role in enhancing our understanding of flow distribution and serves as a key element in the development of predictive models for both flow patterns and their pressure gradients. The techniques used to measure phase hold up (in-situ) are the sampling method, the photograph method, and the intrusive method. The sampling method is trapping the

[*]Mohamed H. Alashker, *Volume and Fluid Flow Metrology Laboratory, National Institute of Standards (NIS), Giza, Egypt*, +201154996921, eng_m.hassn@yahoo.com

immiscible liquids suddenly during the flowing by two quick closing valves (QCV) [6] at a dedicated section in the pipe. Then the fluids in the trapped volume are drained and measured by calibrated volumetric cylinder. This method is well-suited for obtaining steady-state measurements and is not designed for intermittent flow conditions. The photograph method is taking photographs during the experiments and then extracting data of water holdup for CAF. The intrusive or probe method is based on conductivity probes that detect instantaneous fractions. It is less likely to be feasible for heavy oil CAF due to oil adhesion[7].

Shi et al. (2017) [8] performed experiments on the horizontal CAF in a pipeline with a 26 mm inner diameter and around 6.5m length, where the oil viscosity is 3.3Pa.s and the oil density is 905 kg/m^3. They compared their outcomes with models previously published by Arney et al. [9] and also Brauner [10]. These models accurately predicted water holdup when the oil core was centered in the pipe, but overestimated water holdup when the oil core was off-center. For pressure gradient, they reported that the models' predictions did not match their results because the models did not consider oil contamination in the inner wall and off-center flow of the oil.

Several experimental studies on CAF have contributed to our understanding of flow regimes and pressure frictional gradients [11]–[17]. While, there are complexities in measurements of liquid phase holdup at high velocities of two fluids, so only a few investigations have included the liquid holdup measurements [7], [9], [18]. A comprehensive understanding of two-phase flow behavior through horizontal pipelines is vital for accurately predicting flow patterns and pressure gradients, as well as phase holdup predictions. This knowledge is crucial for network design and operational considerations. Computational Fluid Dynamics (CFD) technology can obtain enough details about multiphase flow characteristics compared to experiments.

A study on the simulation of CAF flow through a Venturi and nozzle flow meter using CFD showed that CFD is a reliable tool for predicting CAF flow in pipelines[19]. Kaushik et al. [20] validated the outcomes of simulation of two-phase flow through irregular pipe configuration with the experimental results of Balakhrisna et al. [21]. The results demonstrated a strong agreement concerning the hydrodynamic behavior for CAF. The wave shape simulation has been enhanced by applying VOF scheme in ANSYS FLUENT [22]. Housz et al. [23] and also Ooms et al. [24] numerically studied the Volume of Fluid scheme for simulating horizontal CAF under a wide range of Reynolds number conditions. Ooms et al. [25] modelled numerically heavy oil CAF under assumption that the oil core is solid. Bai et al.[26] performed CFD simulation of laminar CAF of liquids with the same density by assuming axisymmetric interfacial waves and a solid oil core.

With the growth of computer technology, it is growing in popularity. To study the stability of CAF flows, some specialized internal CFD codes have been created to give the right insight and foresight into flow behaviors. In this study, the ANSYS FLUENT 2020R1 was used to study flow characteristics of heavy oil-water CAF pattern with turbulence in the water annulus through a horizontal pipeline. A three-dimensional model of transient isothermal flows was numerically created with applying the VOF method. The transient pressure was numerically calculated and experimentally measured. The predictions of CFD for pressure gradients and oil holdup were validated with experimental results and values of published correlation of holdup.

2. Experimental facility

Experiments on two-phase flow heavy oil-water were performed at the National Institute of Standards (NIS), Egypt. The experimental setup used consists of a closed-loop circuit. The test section consists of an acrylic pipe of 50 mm inner diameter and 6 m length equipped with a fluid lubricant injector nozzle as shown in Figure 1. Six electronic pressure transmitters were installed and distributed equally at distinct positions throughout the test section. The distance between any two successive pressure transmitters is one meter. The test section was equipped with a PT100 temperature sensor at the end, as shown in Figure 1.

Heavy oil (ρ=900 kg/m3; μ=1.35 Pa.s at 25 ◦C) and water were used as the working fluid. The oil flow rate was measured by a calibrated positive displacement meter (manufactured by OMEGA) with an uncertainty of ±0.41% of the reading for flow rates up to 5.5 m³/h. The water flow rate was measured by a calibrated turbine meter (manufactured by Flow Technology) with an uncertainty of ±0.43% of reading for flow rates up to 11 m^3/h. The data acquisition system (LabJack T7) collected all signals from the flowmeters, pressure transmitters, and temperature sensor, and processed them using a software program(LJLogM).

The water and the oil were kept in separate tanks. The water was pumped to the annulus of the lubrication injector nozzle while the oil was pumped into the center of the lubrication injector nozzle and then flowed concurrently through a test section. After the test section, the oil-water mixture was collected in a separation tank, where the two fluids were separated and pumped back to their storage tanks.

The experimental procedures are then as follows: the water was only pumped at maximum value of superficial velocity $u_{w,max}$ and followed by the injection of oil at a fixed value of superficial velocity u_o. The u_w of water is decreased at each run until the lowest value $u_{w,min}$ is reached. After steady-state conditions were achieved, the temperature, pressure, and flow rate were recorded. The pipe was flushed with water and compressed air before each test to mitigate the fouling of viscous oil on the inner wall of the pipe.

2.1. Governing parameters

The governing parameters which are related to the current study are as follows:

The superficial velocity, u_i (m/s), is the mean velocity which is calculated by dividing the flow rate (Q_o, Q_w) of each single-phase by the cross-section area (A) of the pipe.

$$u_o = \frac{Q_o}{A};\ u_W = \frac{Q_w}{A} \quad (1)$$

$$u_m = u_o + u_w \quad (2)$$

The velocity of the mixture denoted as u_m, is the combined result of the superficial velocity for the heavy oil phase with the water phase.

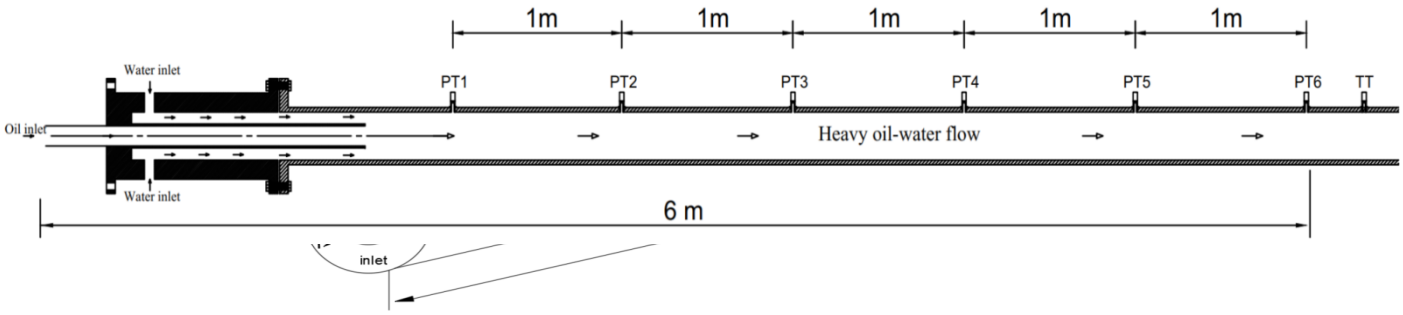

Figure 2: Schematic diagram of model geometry.

The oil input volume fraction ε_o is expressed as

$$\varepsilon_o = \frac{Q_o}{Q_o + Q_w};\ \ \varepsilon_w = 1 - \varepsilon_o \qquad 3$$

The volume-averaged oil holdup H_o is defined as

$$H_o = \frac{V_o}{V_{tot}};\ \ H_w = 1 - H_o \qquad 4$$

Where: V_{tot} is the volume trapped within a dedicated section and V_o is the volume occupied by the oil.

3. CFD Model

3.1. Modeling Details

CFD modeling, meshing, and simulation were performed using the ANSYS FLUENT software. A three-dimensional model has been created to study core annular flow. The geometry of the presented three-dimensional problem is shown in Figure 2. The model having a 0.05 m main diameter and 0.021 m inlet diameter of oil core (same as in our experimental work) and length of 2.5 m was considered for analysis in the present computational work to save the time-consumption of CFD simulation.

Figure 3 depicts a close-up view of the mesh at the two fluids' inlet. The mesh becomes increasingly finer as it gets closer to the pipe wall. The first cell next to the pipe wall is small enough, with a y+ less 5 (y+ is a dimensionless distance that accurately represents the height of the computational cell nearest to the pipe wall in a CFD simulation). The convergence criterion for a grid independence test is the threshold that dictates when the simulation results are considered sufficiently accurate and not significantly affected by changes in the mesh size. To apply the convergence criterion, the geometry was meshed using different numbers of cells between 61760 and 577854 hexahedral cells. The pressure gradients were obtained corresponding to each number of cells at 0.8 m/s and 1.02 m/s superficial velocities of oil and water respectively as shown in Table 1. The pressure gradient gradually increases until it reaches 733 Pa/m at 363020 cells and then the increases are considerably small. It is found that the 577854 cells led to 0.4% difference compared to the 363020 cells. It is concluded that the final mesh of 577854 cells is sufficient for the acceptable accuracy of the solution.

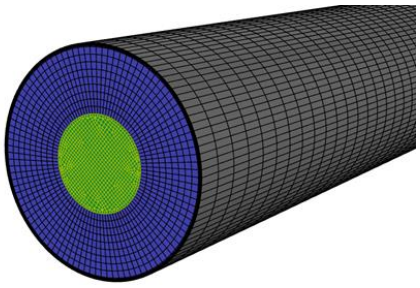

Figure 3: Mesh of partial geometry (blue and green colours refer to water and oil regions respectively)

3.2. Mathematical model

The application of the Volume of Fluid (VOF) technique as a multiphase model in ANSYS FLUENT 20R1 was employed. This technique is well-suited for simulating heavy oil-water core-annular flow because the two phases do not mix and are separated by a thin interface that is similar in length to the diameter of pipe

The measured pressure gradient of experiment is 785 Pa/m [19],

Table 1. Grid independence study of model geometry for u_o=0.8 m/s and u_w=1.02m/s.

Number of mesh	Pressure gradient (pa/m)	Relative error to experiment (%)
61760	703	-10.4
175532	721	-8.2
363020	733	-6.6
577854	737	-6.2

[27] [29]. The VOF technique has the capability to simulate multiple fluids by solving a single set of momentum equations [30]. In this model, the assumptions include transient flow, the presence of an immiscible liquid pair, isothermal conditions without mass heat transfer, and without phase exchange (no interpenetration. The governing equations for mass and momentum, describing the flow of oil-water, are presented as follows:

$$\frac{\partial(\rho)}{\partial t}+\rho\left(\frac{1}{r}\frac{\partial(rv_r)}{\partial r}+\frac{1}{r}\frac{\partial v_\theta}{\partial \theta}+\frac{\partial v_z}{\partial z}\right)=0 \quad (5)$$

$$(\boldsymbol{Z-momentum})\ \frac{\partial}{\partial t}(\rho v_z)+\rho\left(v_r\frac{\partial v_z}{\partial r}+\frac{v_\theta}{r}\frac{\partial v_z}{\partial \theta}+v_z\frac{\partial v_z}{\partial z}\right)$$
$$=-\frac{\partial p}{\partial z}+\mu\left[\frac{1}{r}\frac{\partial}{\partial r}\left(r\frac{\partial v_z}{\partial r}\right)+\frac{1}{r^2}\frac{\partial^2 v_z}{\partial \theta^2}+\frac{\partial^2 v_z}{\partial z^2}\right]+\rho g_z+f_z \quad (6)$$

$$(\boldsymbol{r-momentum})\ \frac{\partial}{\partial t}(\rho v_r)+\rho\left(v_r\frac{\partial v_r}{\partial r}+\frac{v_\theta}{r}\frac{\partial v_r}{\partial \theta}-\frac{v_\theta^2}{r}+v_z\frac{\partial v_r}{\partial z}\right)$$
$$=-\frac{\partial p}{\partial r}+\mu\left[\frac{1}{r}\frac{\partial}{\partial r}\left(r\frac{\partial v_r}{\partial r}\right)-\frac{v_r}{r^2}+\frac{1}{r^2}\frac{\partial^2 v_r}{\partial \theta^2}-\frac{2}{r^2}\frac{\partial v_\theta}{\partial \theta}+\frac{\partial^2 v_r}{\partial z^2}\right]+\rho g_r+f_r \quad (7)$$

$$(\theta-\boldsymbol{momentum})\ \frac{\partial}{\partial t}(\rho v_\theta)+\rho\left(v_r\frac{\partial v_\theta}{\partial r}+\frac{v_\theta}{r}\frac{\partial v_\theta}{\partial \theta}+\frac{v_r v_\theta}{r}+v_z\frac{\partial v_\theta}{\partial z}\right)$$
$$=-\frac{1}{r}\frac{\partial p}{\partial \theta}+\mu\left[\frac{1}{r}\frac{\partial}{\partial r}\left(r\frac{\partial v_\theta}{\partial r}\right)-\frac{v_\theta}{r^2}+\frac{1}{r^2}\frac{\partial^2 v_\theta}{\partial \theta^2}+\frac{2}{r^2}\frac{\partial v_r}{\partial \theta}+\frac{\partial^2 v_\theta}{\partial z^2}\right]+\rho g_\theta+f_\theta \quad (8)$$

In VOF algorithm, solves a single set of momentum equations and then tracks the interface between the water and the oil phases by finding solution of following conservation equation of oil volume fraction (α_o), assuming the phase density is constant, which is given by:

$$\frac{\partial(\rho_o\alpha_o)}{\partial t}+\rho_o\alpha_o\left(\frac{1}{r}\frac{\partial(rv_r)}{\partial r}+\frac{1}{r}\frac{\partial v_\theta}{\partial \theta}+\frac{\partial v_z}{\partial z}\right)=0 \quad (9)$$

The marker α has a value from 0 to 1 and is described as the volume fraction of oil and water as:

$$\alpha=\begin{cases}0 & \text{Water} & \text{(The cell is devoid of the oil phase)}\\ 1 & \text{Oil} & \text{(The cell is filled with oil phase)}\\ 0<\alpha<1 & \text{Interface} & \text{(The cell hosts the interface between two phases)}\end{cases}$$

After calculating the volume fraction of oil, we determine the volume fraction of water α_w in each cell using the following relationship:

$$\alpha_o+\alpha_w=1;\ \text{where}\ \alpha_o=\alpha \quad (10)$$

Depending on the phase volume fractions in the cell, the average density (ρ) and viscosity (μ) of two fluids in the cell are determined as:

$$\rho=\rho_o\alpha_o+\rho_w\alpha_w \quad (11)$$

$$\mu=\mu_o\alpha_o+\mu_w\alpha_w \quad (12)$$

The group of k-ε models is commonly used in practical engineering applications because they converge quickly and require relatively little memory. Realizable k–ε (RKE) model is particularly well-suited for simulating flows with rotation, boundary layers, and separation [31]. The predictions of the RKE model and shear stress transport (SST) k–ω model were compared with the experimental pressure gradient of two-phase flow by [19]. As a result, the RKE turbulence model displayed a superior prediction. Consequently, we selected the Realizable k–ε model the turbulence model for present simulation. Its mathematical derivations in all details can be seen in [31].

3.3. Initial and boundary conditions

Adequate boundary conditions that describe the fluid flow physics of oil-water must be defined rightly in the CFD solver. Pressure-based segregated algorithms and explicit VOF scheme were selected to solve 3D transient isothermal two-phase flow. The two fluids of oil and water were used as a working fluid.

We assume that the velocity of each fluid is uniform and defined at the inlet respective position as ($U_{inlet}=U_w$ and $U_{inlet}=U_o$) are attributed both for oil and water. The water is injected firstly from the annulus region to the computational domain until the domain is fully filled, then the two fluids are separately injected into the domain, whereas the oil is injected from the core region. These arrangements as the same in the experimental conditions. The wall contact angle was 90◦ as a default in the setting of Ansys Fluent.

For the pipe wall, the wall is stationary, no-slip conditions are implemented and it is assumed that no fluid penetration occurs at the walls (U = 0, at r = 0.05 m for $0°\le\theta\le360°$) along the model. As for the outlet, we assumed an atmospheric or zero-gauge pressure for the outlet gauge pressure (P_{out} = 0). The centerline is set to be the z-axis, where the origin starts from the inlet of a model.

The hydraulic diameter (D) and turbulence intensity (I) are specified according to Guide of Fluent User [30], that is $I_w=0.16\,Re_w^{-0.125}$ Where Re_w is Reynolds number of the water phase, while $I_o=0$ for oil phase [32]. The convergence criteria were set at residual error $\varepsilon_{err}\le10^{-3}$ for continuity equations, momentum equations, static pressures, volume fluid fraction equations and turbulence equations. The time step size used in all simulations is 0.00015 s in accordance with the Courant number which is defined as a number to evaluate the time step transient simulation requirements at a certain velocity for a specified mesh size.

4. Results and discussion

4.1. Time-dependent pressure and generated flow regimes

The present experiments and CFD simulations focused on a horizontal CAF regime in the pipe. The flow within the water annulus exhibited turbulence, characterised by water Reynolds numbers of approximately 100×10^3. Conversely, the flow of oil core remained in the laminar region. Consequently, the regimes of Core-Annular Flow (CAF) reside within the realm of turbulent flow.

Figure 4 shows the monitored time-dependent pressure for the experiment (PT3 sensor) and CFD simulation at 2.4 m from the inlet for different input water fractions with fixed value of oil superficial velocity (u_o= 0.8 m/s). It can be seen that the transient pressure for low input water fraction (15.6%) fluctuated experimentally between 0.67 kPa and 16.3 kPa as shown in Figure (4. a) and the average CFD simulation was about 7.39 kPa. While for high input water fraction (56.6%), oscillated experimentally from 1 kPa to 22 kPa with an average reading of 8.8 kPa as shown in Figure (4. b) and the average CFD simulation was about 9 kPa. The augmentation in water volume fraction does not contribute to the enhancement of core-annular

flow stability; however, it does result in an escalation of the total oil-water flow rate. This augmented flow rate consequently induces an elevation in the pressure gradient across all oil superficial velocities [33].

From the comparison of transient pressure between the experimental results and CFD data. It is noted that the transient pressure fluctuated significantly for experimental results in a higher way compared to that obtained from the CFD simulation. A possible explanation for this occurrence could be the adherence of oil in the pipe's inner wall following the flushing process with water and pressurized air during the experiment. In general, the experimental results and CFD data are taken after steady state conditions are achieved.

Figure 5 shows the CFD predicted contour plots of oil volume fraction for the different input water volume fractions at fixed value of oil superficial velocity (u_o= 0.8 m/s). Figure 5a shows the film of thin water at the upper part and a wavy interface is observed in the CFD due to the density variation beside the significant velocity difference between oil and water across the interface, which destabilizes it. Additionally, the oil core exhibits movement resembling that of a solid body (oil core does not deform or partially break into lumps). These lead to the formation of Kelvin-Helmholtz instability, which is characterised by the waves along the interface.

With the increase ε_w from 15.6% to 56.6%, Figure 5b shows in CFD simulation a thicker bottom water film without the wavy interface. However, experimental observations reveal flow patterns contained oil dispersion at the lower section of the oil core, along with observable oscillations in the entirety of the oil core.

The flow regime was predicted numerically and observed experimentally to change from semi-concentric to eccentric core-annular flow as the water fraction increased from 15.6% to 56.6%. In general, the CFD Simulations predict reasonably well and indicate that for a high oil viscosity, the VOF model may forecast flow patterns in oil-water flow with good degree of sufficiency [32].

Figure 6 presents sequential pictures depicting the development of the oil core across the computational domain at various time intervals for the given case u_o= 0.8 m/s and ε_w =15.6%. It is observed that a thin film of water wets the inner wall of the pipe, which develops an annular flow. The water film at the top is thinner than at the bottom due to the gravitational effect caused by the density variation between two fluids, whereby the oil is less dense than the water. This film of water is achieved throughout the whole domain in less than 2.6 seconds, demonstrating how quickly the condition progresses towards a fully core annular flow, however, instabilities and small waves were generated.

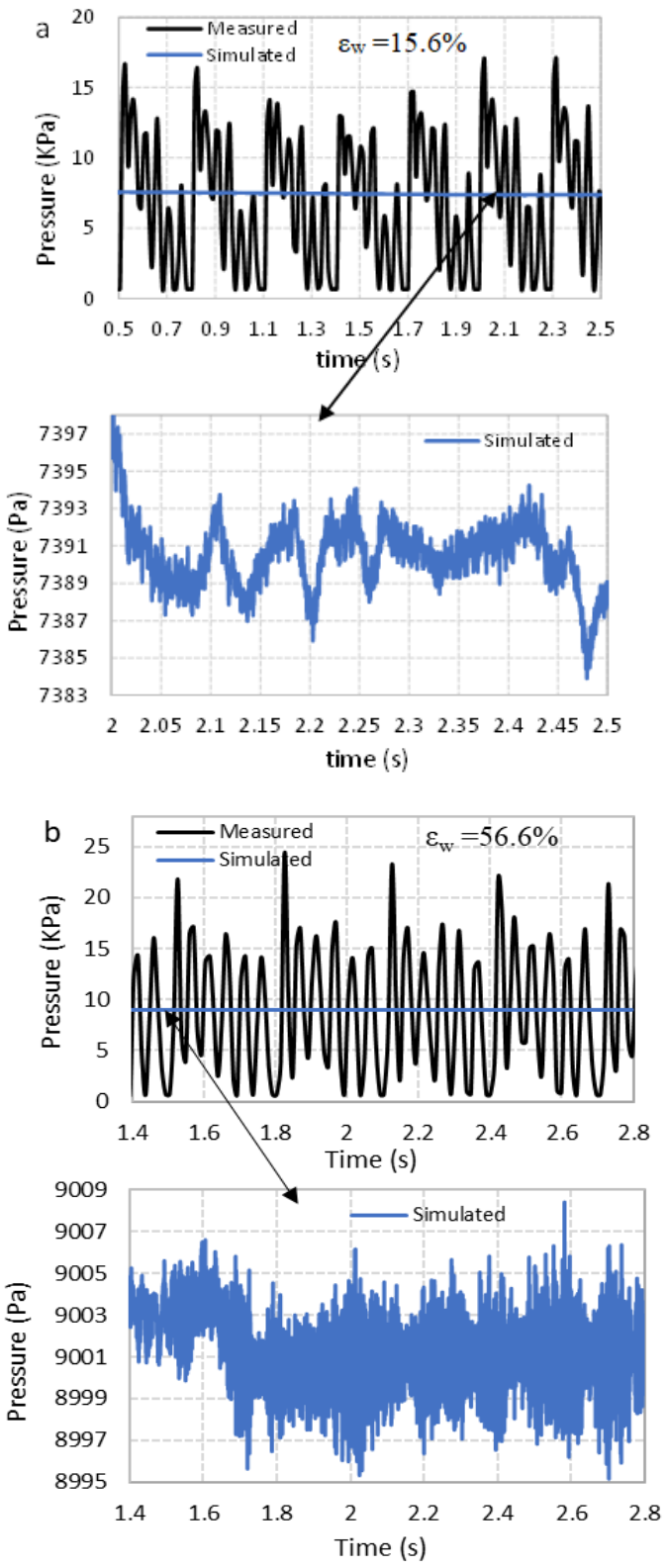

Figure 4: Transient pressure for experiment and CFD simulation a) ε_w=15.6%, b) ε_w=56.6% at fixed u_o= 0.8 m/s.

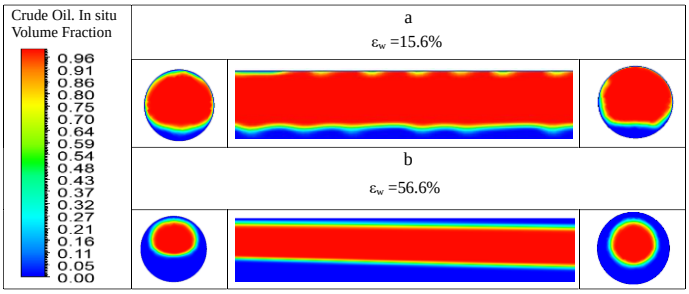

Figure 5: The CFD predicted contour of oil volume fraction for (a) ε_w=15.6% and (b)ε_w=56.6% at fixed value of oil superficial velocity (u_o= 0.8 m/s). The colour red corresponds to the representation of oil and the colour blue corresponds to the representation of water.

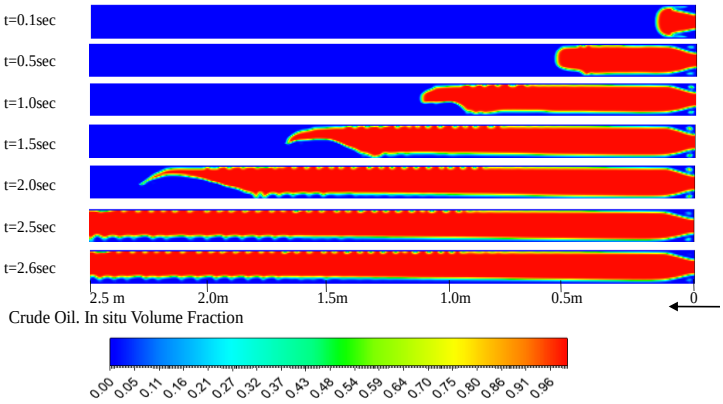

Figure 6: Development of the oil phase over the intervals time of simulation, for flow condition corresponding to u_o= 0.8 m/s, ε_w=15.6% (Water initialization). The colour red corresponds to the representation of oil and the colour blue corresponds to the representation of water.

4.2. Pressure gradients

The pressure gradient was measured for different oil and water flow rates. The CFD calculations were performed along the z-axis direction for a 2.5 m distance. The z-axis is a coordinate axis as shown in Figure 2, which is used to represent the direction of fluid flow along a pipe, indicating positions along the pipe's length, parallel to the flow path.

A direct comparison between the measured pressure gradients and the predictions of CFD is presented in Figure 7. It is observed that the CFD values underpredict the measured pressure gradient. Apart from CFD and instrumentation accuracy, this difference is probably the result of a poor evaluation of oil contamination on tube wall, as there is oil stuck to the inner wall of the tube observed in the experiments due to the oil core eccentricity and also due to the system shutdown to change operating conditions, despite the test section was flushed.

It is demonstrated that the CFD values underpredict the experimental results with a maximum deviation of -25% and the average relative error is around -14.7%. The dispersion of CFD predicted points is observed, with a standard deviation of about ±17.6%.

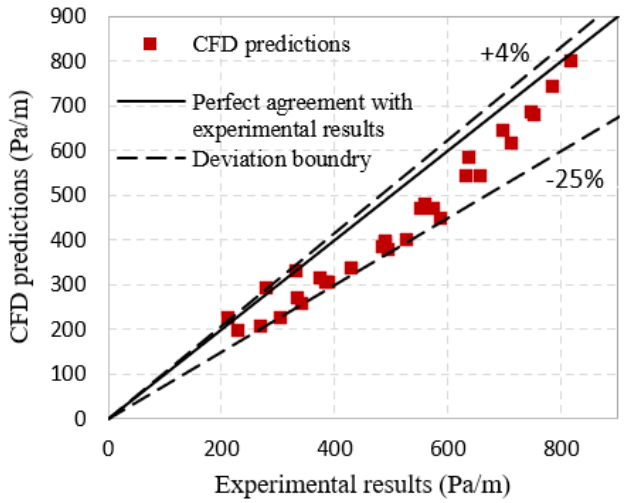

Figure 7: Comparison of the measured pressure gradients with the CFD predictions

4.3. Volume-averaged oil holdup

The average oil holdup measurements within a fully developed region align with the volume-averaged oil holdup values derived from CFD calculations. Due to the unavailability of current experimental oil holdup measurements, the oil holdup derived from CFD $H_{o\,(CFD)}$ was compared with that estimated by Arney correlation $H_{o\,(Arney)}$ due to its accurate prediction among the proposed prediction correlations by different researchers [34].

When oil and water are concurrently transported together through a horizontal pipeline, the in-situ volume fraction of oil during flow varies from the initially input oil volume fraction. The sampling method is the among used techniques to measure phase hold up, which is a basic method. The principle operation of this method is trapping the immiscible liquids suddenly during flowing by two quick closing valves at a dedicated section in the pipe. Then the fluids in the trapped volume are drained and measured by a calibrated volumetric cylinder.

Early research in the 1950s by researchers Charles et al [13] applied the sampling method on oil-water flow for different viscosity oils. Also, Arney et al., and Sridhar et al., conducted measurements of the holdups for heavy oils utilizing a dedicated section equipped with two valves. The phase holdup correlation of Areny is expressed in Equation (11, 12), was checked experimentally and numerically in the previous works [19], [34], [35]. It was found that a good agreement with experimental and numerical data, either in pipes with a uniform diameter or after abrupt changes in pipe diameter.

$$H_{w(Areny)} = \varepsilon_w[1 + 0.35(1 - \varepsilon_w)] \quad 13$$

$$H_{o(Arney)} = 1 - H_{w(Areny)} \quad 14$$

The comparison of CFD $H_{o\,(CFD)}$ with $H_{o\,(Arney)}$ is shown in Figure 8, where $H_{o\,(CFD)}$ was extracted along the pipe from 2 m up to 2.5 m. It is observed that the CFD predictions of oil holdup overestimate the values from correlation of Arney, with a maximum deviation about 15% and the average relative error is around 9.3%. The dispersion of CFD predictions is expressed with a standard deviation of about ±10.7%. The outcomes comparison provides a reasonable consistency.

Table 2 lists the values of input oil fraction for Ho (CFD) and Ho (Arney) at constant oil superficial velocities while varying water superficial velocity. It is demonstrated that the values from both CFD calculations and Arney correlation underestimate the ε_o. As the u_w rises, the relative error of CFD predictions increases. Figure 9 shows the slip ratio of heavy oil-water CAF against ε_w at fixed u_o. It is observed that the average value of the slip ratio (U_o/U_w) is around 1.2, this means that the oil moves faster than water through the pipe.

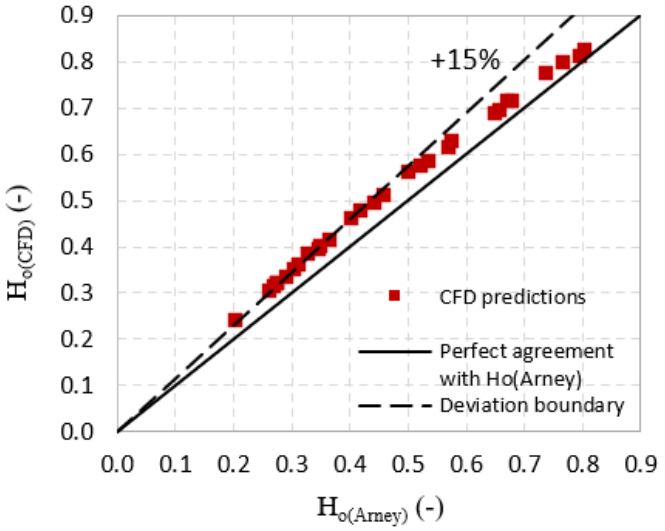

Figure 8: Comparison between the CFD predictions of volume-averaged oil holdup $Ho_{(CFD)}$ and Areny et al. (1993) correlation outcomes $Ho_{(Exp)}$.

Table 2: Comparison between CFD Predictions and Areny estimation of average oil holdup for several fixed superficial velocities of oil.

Case	Oil superficial velocity u_o (m/s)	Water superficial velocity u_w (m/s)	Input oil fraction ε_o	Areny et al (1993) $H_{o\,(Arney)}$	CFD predictions $H_{o\,(CFD)}$	Error[a] (%)
S1-1	0.5	0.123	0.797	0.741	0.772	4.2
S1-2		0.255	0.655	0.576	0.627	8.9
S1-3		0.340	0.588	0.503	0.560	11.4
S1-4		1.265	0.277	0.207	0.237	14.7
S2-1	0.6	0.223	0.721	0.651	0.685	5.3
S2-2		0.374	0.607	0.524	0.572	9.3
S2-3		0.764	0.437	0.351	0.398	13.2
S2-4		1.138	0.343	0.264	0.302	14.4
S3-1	0.7	0.123	0.850	0.805	0.824	2.4
S3-2		0.427	0.620	0.537	0.582	8.4
S3-3		0.611	0.532	0.445	0.494	10.9
S3-4		1.257	0.357	0.276	0.317	14.9
S4-1	0.8	0.144	0.844	0.798	0.801	1.5
S4-2		0.416	0.652	0.573	0.614	7.1
S4-3		0.645	0.548	0.461	0.508	10.2
S4-4		1.308	0.374	0.292	0.333	14.0

a: $\text{Error}\ (\%)\ = \times 100\ \left[(\text{Ho (CFD)} - \text{Ho (Arney)}) \Big/ (\text{Ho (Arney)})\right]$

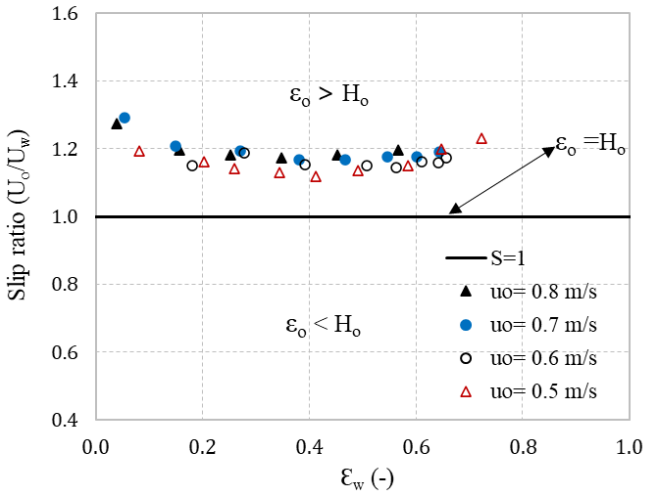

Figure 9: Slip ratio of heavy oil-water CAF against input water volume fraction at fixed oil superficial velocities in a horizontal pipe. The solid line represents the actual oil velocity U_o equal to the actual water velocity U_w

5. Conclusion

A CFD simulation was performed to investigate the flow characteristics of horizontal CAF for heavy oil-water via pipeline, with turbulence in the water annulus. A three-dimensional model of transient isothermal flows for CAF was created with 577,854 mesh elements using CFD code ANSYS FLUENT 2020 R1 applying an explicit VOF scheme. The CAF pattern was determined with varying mixture superficial velocities. The CFD predictions were validated with the experimental data and the published correlation values of phase holdup. The following are the main conclusions of this study:

- The transient pressure fluctuated significantly for the experiments higher than obtained for CFD simulations due to the oil stuck in the inner pipe wall during the experiments. Thicker eccentricity core flow has been observed numerically and consistent with the flow visualization observed experimentally.
- The interfacial waves appeared at low ε_w during the simulation study of the flow. This was due to the assumption that the oil core exhibits movement resembling that of a solid body. As a result, the oil core does not deform or partially break into lumps. Additionally, the density variation beside the significant velocity difference between oil and water across the interface, which destabilizes it. These lead to the formation of Kelvin-Helmholtz instability, which is characterised by the formation of waves along the interface.
- The simulated oil holdup and pressure gradients were found to be in reasonable agreement with Areny's correlation predictions and experimental results, respectively. The maximum deviations observed for pressure gradient and oil holdup were -25% and 15%, respectively. The $Ho_{(CFD)}$ was compared to the values of correlation associated with Arney et al. (1993) because of the experimental measurements for H_o were not available in the present study.
- This investigation further demonstrates that the CFD model may provide useful insight into the horizontal flow of heavy oil-water via pipe and successfully predicting the hydrodynamic behavior of core annular flow at a high level of accuracy.

Conflict of Interest

The authors declare no conflict of interest.

References

[1] K. C. O. Crivelaro, Y. T. Damacena, T. H. F. Andrade, A. G. B. Lima, and S. R. Farias Neto, "Numerical simulation of heavy oil flows in pipes using the core-annular flow technique," *WIT Trans. Eng. Sci.*, vol. 63, pp. 193–203, 2009, doi: 10.2495/MPF090171.

[2] R. . Santos and Lo, "Brazilian Journal of Chemical Engineering - An overview of heavy oil properties and its recovery and transportation methods," *Brazilian J. Chem. Eng.*, vol. 31, no. 03, pp. 571–590, 2014.

[3] R. Martínez-Palou *et al.*, "Transportation of heavy and extra-heavy crude oil by pipeline: A review," *J. Pet. Sci. Eng.*, vol. 75, no. 3–4, pp. 274–282, 2011, doi: 10.1016/j.petrol.2010.11.020.

[4] W. L. Loh and V. K. Premanadhan, "Experimental investigation of viscous oil-water flows in pipeline," *J. Pet. Sci. Eng.*, vol. 147, pp. 87–97, 2016, doi: 10.1016/j.petrol.2016.05.010.

[5] A. Bensakhria, Y. Peysson, and G. Antonini, "Experimental Study of the Pipeline Lubrication for Heavy Oil Transport," vol. 59, no. 5, pp. 523–533, 2004.

[6] G. Oddie, H. Shi, L. J. Durlofsky, K. Aziz, B. Pfeffer, and J. A. Holmes, "Experimental study of two and three phase flows in large diameter inclined pipes," *Int. J. Multiph. Flow*, vol. 29, no. 4, pp. 527–558, 2003, doi: 10.1016/S0301-9322(03)00015-6.

[7] J. Shi, L. Lao, and H. Yeung, "Water-lubricated transport of high-viscosity oil in horizontal pipes: The water holdup and pressure gradient," *Int. J. Multiph. Flow*, vol. 96, pp. 70–85, 2017, doi: 10.1016/j.ijmultiphaseflow.2017.07.005.

[8] J. Shi, L. Lao, and H. Yeung, "Water-lubricated transport of high-viscosity oil in horizontal pipes: The water holdup and pressure gradient," *Int. J. Multiph. Flow*, vol. 96, pp. 70–85, 2017, doi: 10.1016/j.ijmultiphaseflow.2017.07.005.

[9] M. S. Arney, R. Bai, E. Guevara, D. D. Joseph, and K. Liu, "Friction factor and holdup studies for lubricated pipelining-I, experiments and correlations," *Int. J. Multiph. Flow*, vol. 19, no. 6, pp. 1061–1076, 1993.

[10] N. Brauner, "Liquid–liquid two-phase flow," in *In: Hewitt, G.F. (Ed.), Heat Exchanger Design Handbook. Begell House*, 1998.

[11] M. J. McKibben, R. G. Gillies, and C. A. Shook, "Predicting pressure gradients in heavy oil-water pipelines," *Can. J. Chem. Eng.*, vol. 78, no. 4, pp. 752–756, 2000.

[12] M. Mckibben, R. Gillies, C. Pipe, F. Technology, and S. Sanders, "A New Method for Predicting Friction Losses and Solids Deposition during the Water-Assisted Pipeline Transport of Heavy Oils and Co-Produced Sand," in *SPE Heavy Oil Conference-Canada 11-13*, 2013.

[13] B. Grassi, D. Strazza, and P. Poesio, "Experimental validation of theoretical models in two-phase high-viscosity ratio liquid-liquid flows in horizontal and slightly inclined pipes," *Int. J. Multiph. Flow*, vol. 34, no. 10, pp. 950–965, 2008, doi: 10.1016/j.ijmultiphaseflow.2008.03.006.

[14] G. Sotgia, P. Tartarini, and E. Stalio, "Experimental analysis of flow regimes and pressure drop reduction in oil-water mixtures," *Int. J. Multiph. Flow*, vol. 34, no. 12, pp. 1161–1174, 2008, doi: 10.1016/j.ijmultiphaseflow.2008.06.001.

[15] P. Angeli and G. F. Hewitt, "Pressure gradient in horizontal liquid-liquid flows," *Int. J. Multiph. Flow*, vol. 24, no. 7, pp. 1183–1203, 1998, doi: 10.1016/S0301-9322(98)00006-8.

[16] A. C. Bannwart, O. M. H. Rodriguez, C. H. M. De Carvalho, I. S. Wang, and R. M. O. Vara, "Flow patterns in heavy crude oil-water flow," *J. Energy Resour. Technol. Trans. ASME*, vol. 126, no. 3, pp. 184–189, 2004, doi: 10.1115/1.1789520.

[17] A. Abubakar, Y. Al-Wahaibi, T. Al-Wahaibi, A. R. Al-Hashmi, A. Al-Ajmi, and M. Eshrati, "Effect of pipe diameter on horizontal oil-water flow before and after addition of drag-reducing polymer part I: Flow patterns and pressure gradients," *J. Pet. Sci. Eng.*, vol. 153, pp. 12–22, 2017, doi: 10.1016/j.petrol.2017.03.021.

[18] D. Strazza, B. Grassi, M. Demori, V. Ferrari, and P. Poesio, "Core-annular flow in horizontal and slightly inclined pipes: Existence, pressure drops, and hold-up," *Chem. Eng. Sci.*, vol. 66, no. 12, pp. 2853–2863, 2011, doi: 10.1016/j.ces.2011.03.053.

[19] P. Babakhani Dehkordi, L. P. M. Colombo, M. Guilizzoni, and G. Sotgia, "CFD simulation with experimental validation of oil-water core-annular flows through Venturi and Nozzle flow meters," *J. Pet. Sci. Eng.*, vol. 149, no. November 2016, pp. 540–552, 2017, doi: 10.1016/j.petrol.2016.10.058.

[20] V. V. R. Kaushik, S. Ghosh, G. Das, and P. Kumar, "Journal of Petroleum Science and Engineering CFD simulation of core annular fl ow through sudden contraction and expansion," *J. Pet. Sci. Eng.*, vol. 86–87, pp. 153–164, 2012, doi: 10.1016/j.petrol.2012.03.003.

[21] T. Balakhrisna, S. Ghosh, G. Das, and P. K. Das, "Oil-water flows through sudden contraction and expansion in a horizontal pipe - Phase distribution and pressure drop," *Int. J. Multiph. Flow*, vol. 36, no. 1, pp. 13–24, 2010, doi: 10.1016/j.ijmultiphaseflow.2009.08.007.

[22] J. Li and Y. Renardy, "Numerical study of flows of two immiscible liquids at low Reynolds number," *SIAM Rev.*, vol. 42, no. 3, pp. 417–439, 2000, doi: 10.1137/S0036144599354604.

[23] E. M. R. M. Ingen Housz, G. Ooms, R. A. W. M. Henkes, M. J. B. M. Pourquie, A. Kidess, and R. Radhakrishnan, "A comparison between numerical predictions and experimental results for horizontal core-annular flow with a turbulent annulus," *Int. J. Multiph. Flow*, vol. 95, pp. 271–282, 2017, doi: 10.1016/j.ijmultiphaseflow.2017.01.020.

[24] G. Ooms, M. J. B. M. Pourquie, and J. C. Beerens, "On the levitation force in horizontal core-annular flow with a large viscosity ratio and small density ratio On the levitation force in horizontal core-annular flow with a large viscosity ratio and small density ratio," vol. 032102, 2013, doi: 10.1063/1.4793701.

[25] G. Ooms, A. Segal, A. J. Van der Wees, R. Meerhof, and R. V. A. Oliemans, "A theoretical model for core-annular flow of a very viscous oil core and a water annulus through a horizontal pipe," vol. 10, pp. 41–60, 1984.

[26] K. A. N. C. H. A. N. Kelkar, "Direct simulation of interfacial waves in a high-viscosity-ratio and axisymmetric core-annular flow," 1996.

[27] S. Ghosh, G. Das, and P. K. Das, "Simulation of core annular downflow through CFD-A comprehensive study," *Chem. Eng. Process. Process Intensif.*, vol. 49, no. 11, pp. 1222–1228, 2010, doi: 10.1016/j.cep.2010.09.007.

[28] C. W. Hirt, "Volume of Fluid (VOF) Method for the Dynamics of Free Boundaries," vol. 225, pp. 201–225, 1981.

[29] JING SHI, "A STUDY ON HIGH-VISCOSITY OIL-WATER TWO-PHASE FLOW IN HORIZONTAL PIPES," CRANFIELD UNIVERSITY, 2015.

[30] "ANSYS Fluent Theory Guide," *ANSYS, Inc*, 2020. .

[31] H. K. Versteeg and W. Malalasekera, "An Introduction to Computational Fluid Dynamics - The Finite Volume Method," *Fluid flow handbook. McGraw-Hill …*. p. 267, 1995, doi: 10.2514/1.22547.

[32] J. Shi, M. Gourma, and H. Yeung, "A CFD study on horizontal oil-water flow with high viscosity ratio," *Chem. Eng. Sci.*, vol. 229, p. 116097, 2021, doi: 10.1016/j.ces.2020.116097.

[33] J. Jing *et al.*, "Experimental study on highly viscous oil-water annular flow in a horizontal pipe with 90° elbow," *Int. J. Multiph. Flow*, vol. 135, p. 103499, 2021, doi: 10.1016/j.ijmultiphaseflow.2020.103499.

[34] P. Babakhani Dehkordi, A. Azdarpour, and E. Mohammadian, "The hydrodynamic behavior of high viscous oil-water flow through horizontal pipe undergoing sudden expansion—CFD study and experimental validation," *Chem. Eng. Res. Des.*, vol. 139, pp. 144–161, 2018, doi: 10.1016/j.cherd.2018.09.026.

[35] L. P. M. Colombo, M. Guilizzoni, G. M. Sotgia, and D. Marzorati, "International Journal of Heat and Fluid Flow Influence of sudden contractions on in situ volume fractions for oil – water flows in horizontal pipes," *Int. J. Heat Fluid Flow*, vol. 53, pp. 91–97, 2015, doi: 10.1016/j.ijheatfluidflow.2015.03.001.

Nomenclature

A	**Cross sectional area, (m^2)**
d	**Inner diameter, (mm)**
Q_o	**Oil flow rate, (m^3/s)**
Q_w	**Water flow rate, (m^3/s)**
u_o	**Oil superficial velocity, (m/s)**
u_w	**Water superficial velocity, (m/s)**
U	**Average velocity, (m/s)**
U_o	**Actual oil velocity, (m/s)**
U_w	**Actual water velocity, (m/s)**
y^+	**Dimensionless distance, (-)** (y+ is a dimensionless distance that accurately represents the height of the first cell adjacent to the pipe wall in a CFD simulation).
t	**Time, (s)**
p	**Pressure, (N/m^2)**
g	**Gravitational acceleration, (m/s^2)**
v_r, v_θ, v_z	**Instantaneous velocity in the flow field, (m/s)**
$f(f_z, f_x, f_\theta)$	**Interfacial tension force in the flow field, (Kg/m^2s^2)**
I	**Turbulence intensity, (-)**
R_e	**Reynolds number, (-)**
H_o	**Volume-averaged oil holdup, (-)**
H_w	**Volume-averaged water holdup, (-)**
$H_{o(CFD)}$	**The predicted oil holdup by CFD, (-)**
$H_{o(Arney)}$	**The estimated oil holdup by Areny Correlation (-)**
$\Delta P_{ow}/L$	**Pressure gradient of heavy oil-water CAF, (Pa/m)**
V_{tot}	**The trapped volume within a dedicated section, (m^3)**
V_o	**The measured oil volume, (m^3)**
V_w	**The measured water volume, (m^3)**
Z	**longitudinal position from the inlet, (m)**
Greek letters	
μ	**Dynamic viscosity, (cP) or (Pa.s)**
ρ	**Density, (Kg/m^3)**
α	**Phase fraction, (-)**
$\mathcal{E}_o$	**Oil input fraction, (-)**
$\mathcal{E}_w$	**Water input fraction, (-)**
Subscripts	
o	**oil**
w	**water**
Abbreviation	
CAF	**Core-Annular Flow**
CFD	**Computational Fluid Dynamics**
VOF	**Volume of fluid**
QCV	**Quick Closing Valve**